Skeletal development of hallucal tarsometatarsal joint curvature and angulation in extant apes and modern humans

Corey M. Gill [a, b, c], Miriam A. Bredella [a], Jeremy M. DeSilva [c, d, *]

[a] Department of Radiology, Pappas Center for Neuro-Oncology, Massachusetts General Hospital and Harvard Medical School, Boston, MA 02214, USA
[b] Pappas Center for Neuro-Oncology, Department of Neurology and Cancer Center, Massachusetts General Hospital and Harvard Medical School, Boston, MA 02214, USA
[c] Department of Anthropology, Boston University, Boston, MA 02214, USA
[d] Department of Anthropology, Dartmouth College, Hanover, NH 03755, USA

ARTICLE INFO

ABSTRACT

The medial cuneiform, namely the curvature and angulation of its distal facet with metatarsal 1, is crucial as a stabilizer in bipedal locomotion and an axis upon which the great toe medially deviates during arboreal locomotion in extant apes. Previous work has shown that facet curvature and angulation in adult dry-bone specimens can distinguish African apes from *Homo*, and can even distinguish among species of *Gorilla*. This study provides the first ontogenetic assessment of medial cuneiform curvature and angulation in juvenile (n = 68) and adult specimens (n = 102) using computed tomography in humans and extant ape specimens, including *Pongo*. Our data find that modern human juveniles initially have a convex and slightly medially oriented osseous surface of the developing medial cuneiform distal facet that flattens and becomes more distally oriented with age. The same pattern (though of a different magnitude) occurs developmentally in the chimpanzee medial cuneiform, but not in *Gorilla* or *Pongo*, whose medial cuneiform facet angulation remains unchanged ontogenetically. These data suggest that the medial cuneiform ossifies in a distinguishable pattern between *Pongo*, *Gorilla*, *Pan*, and *Homo*, which may in part be due to subtle differences in the loading environment at the hallucal tarsometatarsal joint—a finding that has important implications for interpreting fossil medial cuneiforms.

© 2015 Elsevier Ltd. All rights reserved.

1. Introduction

The medial cuneiform is the most medial distal tarsal bone in the foot, articulating distally with metatarsal 1 and proximally with the navicular. In modern humans, the medial cuneiform is thought to reach adult morphology by six years of age (Scheuer and Black, 2000). Its articulation with the hallux makes the medial cuneiform an essential part of the abduction and grasping mechanism during arboreal locomotion in extant apes and of the propulsive mechanism in *Homo*. The medial cuneiform further contributes to the transverse arch of the foot, along with the intermediate and lateral cuneiforms and cuboid. Moreover, the medial cuneiform serves as a medial attachment site for tibialis anterior, which is crucial for foot inversion, as well as an attachment site for peroneus longus, which everts the foot.

Scholars have long recognized that the adducted hallux is a unique characteristic of the human foot when compared to other primates (Tyson, 1699; Wood Jones, 1916; Keith, 1923; Weidenreich, 1923; Gregory, 1928; Keith, 1929; Schultz, 1930, 1934; Midlo, 1934; Morton, 1935). Schultz (1930, 1934), in particular, noted that the morphology of the medial cuneiform was critical for assessing the relative opposability of the hallux and attempted to quantify both the orientation and curvature of the facet in different species of apes and humans. However, application of these approaches to the fossil record was limited by paucity of hominin medial cuneiforms or first metatarsals (but see Day and Napier, 1964; Lewis, 1972).

Following the recovery and study of a large collection of pedal remains from Hadar, Ethiopia (Latimer et al., 1982), Latimer and Lovejoy (1990) completed the first detailed analysis of medial cuneiform morphology in *Australopithecus (Au.) afarensis*. Using sectioned casts from dry-bone adult specimens of *Pan*, *Gorilla*, and *Homo*, they found that the angular orientation of the distal facet with metatarsal 1 was most oblique in *Pan* specimens with *Homo*

* Corresponding author.
  E-mail addresses: cmgill@mgh.harvard.edu (C.M. Gill), mbredella@mgh.harvard.edu (M.A. Bredella), jeremy.m.desilva@dartmouth.edu (J.M. DeSilva).

having an orientation near 90°. With this measurement, they determined that the 3.2 Ma A.L. 333-28 medial cuneiform assigned to *Au. afarensis* was within the range of variation in modern humans. They further identified differences in the curvature of the distal facet of the medial cuneiform. Latimer and Lovejoy (1990) found that *Pan* had the highest degree of curvature, which they associated with the ability for hallucal abduction and opposability at the tarsometatarsal joint. The more flattened surface of the distal medial cuneiform facet in modern humans was argued to be associated with an increase in the efficiency of the propulsive bipedal push-off mechanism and a decrease in relative mobility at the joint. In the A.L. 333-28 specimen, there was heightened curvature compared to modern humans, which was interpreted as evidence that peroneus longus served as a plantarflexor in the absence of a derived triceps surae. This interpretation has been challenged and the "markedly convex" (Latimer et al., 1982) facet of the A.L. 333-28 medial cuneiform (Stern and Susman, 1983; Susman, 1983; Susman et al., 1984; Deloison, 1992; Berillon, 1999), along with anatomies of the first metatarsal (Proctor, 2010) and the Laetoli footprints (Bennett et al., 2009), have been interpreted as evidence that *Au. afarensis* may have retained some grasping ability with its big toe.

Interpretations of the StW 573 ("Little Foot") medial cuneiform have likewise varied. Originally described as possessing a moderately divergent hallux (Clarke and Tobias, 1995), others have found little evidence for grasping potential in this South African australopith (Harcourt-Smith, 2002; Harcourt-Smith and Aiello, 2004; McHenry and Jones, 2006; Lovejoy et al., 2009).

New methodology has also contributed to our understanding of medial cuneiform morphology in apes and humans. Tocheri et al. (2011) and Solhan (2011) acquired 3D (three-dimensional) models of medial cuneiforms using computed tomography and surface scanning to quantify angulation and curvature of the distal medial cuneiform facet in hominoids. In particular, Tocheri et al. (2011) examined different *Gorilla* species and subspecies to test observations of intrageneric differences in medial cuneiform morphology originally made by Schultz (1930, 1934). They determined that the more arboreal western gorilla has a more curved and medially oriented distal facet, supporting the notion that both measurements can be potentially diagnostic in differentiating degree of arboreality in extant ape populations.

These and other (e.g., Gomberg, 1981; Berillon, 1999; Harcourt-Smith, 2002; McHenry and Jones, 2006) studies established the significance of both angulation and curvature of the distal medial cuneiform facet as functionally informative morphologies in adult apes and humans. How these anatomies develop ontogenetically, however, is entirely unknown. While most ontogenetic studies in paleoanthropology have focused on the skull and/or neurocranium (e.g., Zollikofer and Ponce de León, 2013), an ontogenetic characterization of the postcranium can yield important functional insights into individual behavior (Ward, 2002) and has been used to interpret phalangeal curvature (Richmond, 1998), knuckle-walking adaptation in the apes (Kivell and Schmitt, 2009), and the hominin shoulder (Green and Alemseged, 2012), leg (Tardieu, 2010), and knee (Tardieu, 1999; Shefelbine et al., 2002; Glard et al., 2005). Here, we apply this same approach to the hominoid first tarsometatarsal joint. These data may reveal how functionally critical aspects of adult pedal skeletal morphology actually form in apes and humans and could eventually be useful for interpreting pedal material from juvenile hominins (e.g., Alemseged et al., 2006) and hominoids (e.g., Napier and Davis, 1959; Dunsworth, 2006).

In this study, we test the null hypothesis that there is no significant alteration in bony curvature or angulation of the hallucal tarsometatarsal joint from birth through adulthood in extant ape and modern human medial cuneiforms. Using high-resolution computed tomography (CT), we quantify these measures in juvenile and adult *Pongo*, *Gorilla*, *Pan*, and *Homo*. In addition to characterizing the ontogenetic development of these morphologies, this study examines interspecific differences in morphology of the first tarsometatarsal joint across apes and humans and uses these data to re-interpret fossil medial cuneiforms (A.L. 333-28, StW 573, OH 8) from Plio-Pleistocene hominins.

2. Material and methods

2.1. Specimen selection

The study was approved by the Partners Healthcare Inc. Institutional Review Board and was Health Insurance Portability and Accountability Act compliant. A retrospective search was performed for foot computed tomography (CT) imaging obtained at Massachusetts General Hospital from January 2000 to January 2013 in subjects who were less than 21 years of age. Exclusion criteria included subjects with gross osteogenic deformity, fracture, or abnormality of the medial cuneiform or the adjacent tarsal bones. CT examinations from 46 feet were chosen that met the inclusion criteria. These included three scans per age group from age 9 to 20, two scans for ages 5 and 7, and one scan for ages 1, 2, 3, 4, 6, and 8. Age at time of scan was recorded for each subject.

Dry-bone medial cuneiforms were collected from wild-shot ape specimens from the Museum of Comparative Zoology (MCZ) at Harvard University and the American Museum of Natural History (AMNH) in New York (Table 1). All extant ape specimens had an associated skull cataloged with the medial cuneiforms at their respective museums. Stage of tooth eruption by visual inspection for all specimens was recorded; extant ape adults were defined by complete third molar eruption. Adult samples in *Homo* include specimens with absolute age greater than 17 years old. Dorso-plantar height of the medial cuneiform was used as a proxy for age given the different developmental schedules of the different species examined in this study.

High-quality research casts of A.L. 333-28 (*Au. afarensis*) and 3D surface scans (Next Engine scanner) of the original specimens OH 8 and StW 573 were used in this analysis (Table 2). Ten dry-bone adult *Homo* medial cuneiforms (Boston University biological anthropology laboratory) were also included in the specimen cohort. Because there were no significant differences ($p > 0.1$, all values) when comparing results of curvature or angulation between the adult *Homo* in vivo CT scans and the 10 additional dry-bone adult medial cuneiforms, these data were pooled in all subsequent analyses.

2.2. CT imaging

In vivo CT imaging of human subjects was performed using a GE LightSpeed Pro 16 scanner (General Electric, Milwaukee, WI): slice

Table 1
Medial cuneiforms examined in this study.

Species	Juvenile	Adult	Total
Gorilla gorilla	5	36	41
Pan troglodytes	20	36	56
Pongo pygmaeus	6	7	13
Homo sapiens	37	20	57
Total	**68**	**99**	**167**

In the extant apes, specimens were separated into juveniles and adults based on corresponding tooth eruption of the associated cranium. In *Homo*, juveniles were identified as younger than 18 years of age at time of CT.

Table 2
Hallucal tarsometatarsal joint morphology in hominin fossil medial cuneiforms.

	A.L. 333-28	OH 8	StW 573
Species	*Australopithecus afarensis*	*Homo habilis?* *Australopithecus boisei?*	*Australopithecus* sp.
Radius of curvature (cm)	1.01	1.50	1.51
Metatarsal 1 facet angulation (degrees)	94.0	104.8	103.7
Curvature index (%)	10.0	13.0	9.3

thickness 2.5 mm, 120 kV tube voltage, average tube current-time 300 mAs.

Dry-bone and casts of medial cuneiforms were scanned with a Planmed Verity (Planmed Oy, Helsinki, Finland) CT scanner. All specimens were scanned using a standard protocol of 400 μ slice thickness, 90 kV tube voltage, average tube current-time 3.8 mAs. Scans were completed under the supervision of a board certified musculoskeletal radiologist to assure accuracy and proper technique.

2.3. Anatomical measurements

Because CT was used, soft tissue and cartilage were not captured within the analyzed images. Therefore, measurements were only taken on the osteochondral boundary (if juvenile) or subchondral joint surface of the medial cuneiforms. Residual soft tissue, including fur and skin, especially in cases where articulated extant ape specimens were used, as well as cartilage that could have adhered to the medial cuneiform surface, did not influence the reliability of the captured images. Juvenile specimens that did not have an ossified, either completely or in part, medial cuneiform were excluded from this study, as were medial cuneiforms from individuals young enough that they did not have a recognizable form with clear articular surfaces and defined edges with non-articular regions of the bone.

Measurements were performed in a Picture Archiving and Communication System (PACS) viewer (OsiriX software, version 5.8.5; Pixmeo SARL, Bernex, Switzerland). Before measurements were taken, a 3D surface model was rendered and viewed alongside 2D tri-planar orthogonal images for visual reference and verification (Fig. 1). 3D surface rendering allowed for the most precise point placement possible of facet edges on all specimens (Fig. 2).

Radius of curvature of the distal facet was measured using a circle ROI tool on axial images. The measurement was taken at the transverse slice corresponding to the middle of the navicular facet. The circle was fitted so that the approximate maximum number of points along the facet touched the circular edge. Radius of curvature was recorded in centimeters. We employed an ontogenetic sequence approach to characterize how the curvature of the first metatarsal facet on the medial cuneiform changed with growth in apes and humans. However, because curvature may be expected to reduce with increasing size (see Dunn et al., 2014), we also standardized the radius of curvature by the maximum dorsoplantar height of the bone, recorded on the mid-sagittal slice.

A curvature index was also used to quantify radius of curvature of the medial cuneiform following the techniques described by Latimer and Lovejoy (1990), using transverse images at the level of the middle of the navicular facet to create a reference line from the medial and lateral edges of the distal facet (line B). A perpendicular bisector was created from this reference line to the distal apex of the distal facet (line A). Ratio $(A/B) * 100^2$ is reported as curvature index in percentage.

Medial angulation in degrees of the distal facet was quantified following the techniques described by Latimer and Lovejoy (1990), using transverse images at the level of the middle of the navicular facet by placing points on the lateral edge of the navicular facet as well as on the medial and lateral edges of the distal facet. An angulation tool was used to connect these points to yield medial angulation in degrees.

2.4. Statistical analysis

Statistical analyses were calculated using JMP Pro (v. 11; SAS Institute, Cary, NC). Variables were tested for normality of distribution using the Shapiro–Wilk test. All variables were log-transformed. The *t*-test was used to detect differences between juvenile and adult groups for all measured variables. Multiple comparisons of interspecies variables were performed with the Tukey–Kramer method. $p < 0.05$ was used to denote significance, while $0.05 \leq p < 0.1$ was used to denote a trend. Data are presented as mean ± standard deviation, unless otherwise specified.

3. Results

The distal facet on the human medial cuneiform flattens ontogenetically. There is a strong relationship ($R^2 = 0.78$) between distal curvature and age at time of CT scan (Fig. 3), and between curvature and the dorsoplantar height of the bone ($R^2 = 0.48$). Likewise, the facet flattens as the medial cuneiform grows in the apes (Fig. 4a), with a statistically significant relationship ($p < 0.001$, all values) between facet curvature and dorsoplantar height in *Pan* ($R^2 = 0.60$), *Gorilla* ($R^2 = 0.70$), and *Pongo* ($R^2 = 0.65$). However, the slopes of these lines differ considerably, indicating a much steeper decline in facet curvature in humans (m = 2.1), than in the apes (m = 0.66–0.86).

Facet orientation did not change ontogenetically in *Gorilla* or *Pongo* (Table 3), but decreased slightly with increasing size in both
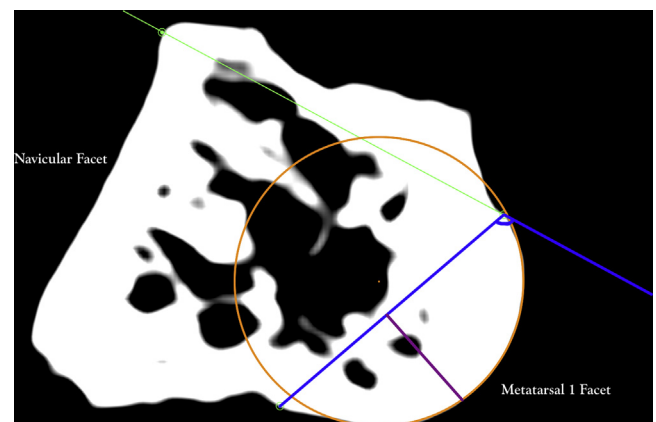

Figure 1. Transverse CT image of the medial cuneiform at the level of the mid-navicular facet with visualization of radius of curvature (orange circle), curvature index (pink and intraosseous blue lines), and metatarsal 1 facet angulation (blue angle) methodologies. The green line represents a baseline for metatarsal 1 facet angulation connecting the lateral edge of the navicular facet and the lateral edge of the metatarsal 1 facet. (For interpretation of the references to color in this figure legend, the reader is referred to the web version of this article.)
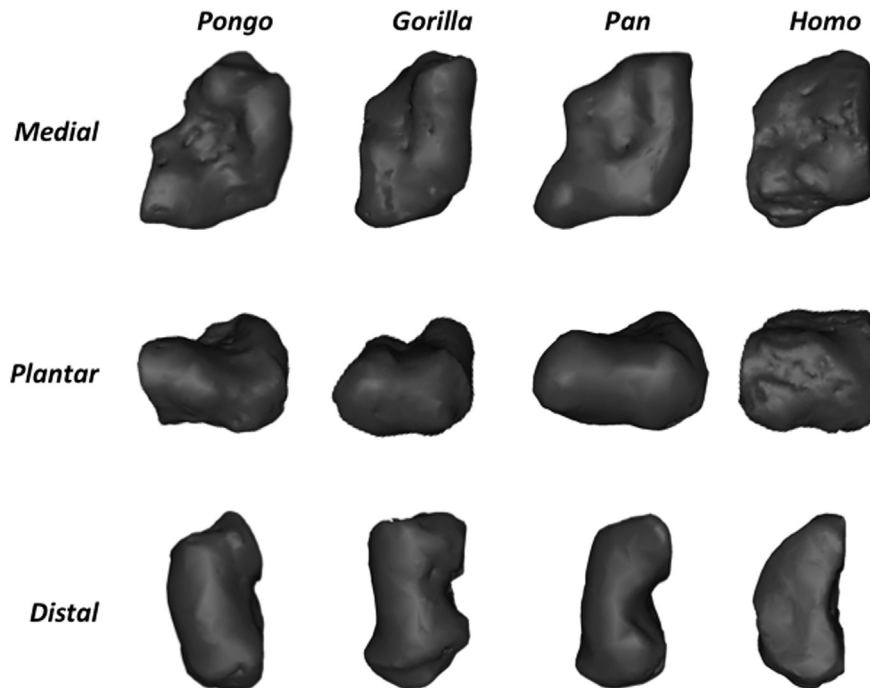
Figure 2. 3D CT rendering of medial cuneiform specimens with medial (row 1), plantar (row 2), and distal (row 3) views present. For rows 1 and 2, the navicular facet (proximal) is left, and metatarsal 1 facet (distal) is right.

Pan ($R^2 = 0.08$) and *Homo* ($R^2 = 0.09$; $p < 0.05$ for both; Table 3; Fig. 4b. Facet orientation also decreased with age treated as a continuous variable in Homo ($R^2 = 0.106$; Fig. 3) as well as categorically in Pan and Homo ($p < 0.05$ for both).

When treated dichotomously (juvenile vs. adult), absolute curvature differed with statistical significance ($p < 0.05$) for *Homo*, *Pan*, and *Gorilla*, with the facet of adults flatter than those of juveniles (Table 3; Fig. 5a). This result appears to be a product of size in the apes, as there is no statistically significant difference in curvature between the adults and the juveniles when standardized by the

dorsoplantar height of the medial cuneiform (Fig. 5b). In humans, however, this relationship remains significant with the facet of adults significantly flatter than that of juveniles whether comparing raw or size-standardized values (Table 3; Figs. 3–5).

Results of interspecific comparison between adult medial cuneiforms reveal a significant difference in radius of curvature and facet orientation (both $p < 0.0001$) in humans compared to the apes. There are interspecific differences within the apes as well, with *Gorilla* adult specimens having a relatively flatter facet ($p = 0.04$) than *Pan*. However, no significant difference in curvature
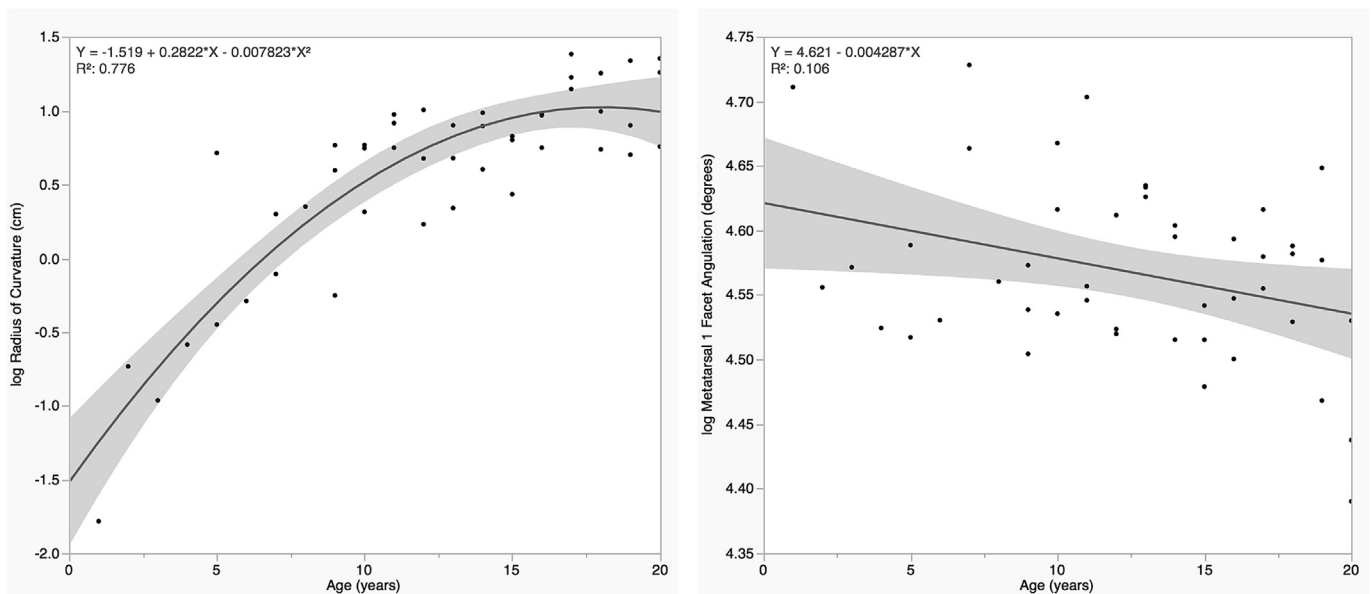

Figure 3. Bivariate regression analysis between measurements of curvature (left) and angulation (right) against age in *Homo*, depicting rapid flattening and gradual decreasing medial deviation of the metatarsal 1 facet between birth and twenty years of age. Shaded region adjacent to regression line represents 95% confidence interval. Line equation and R^2 values are presented.
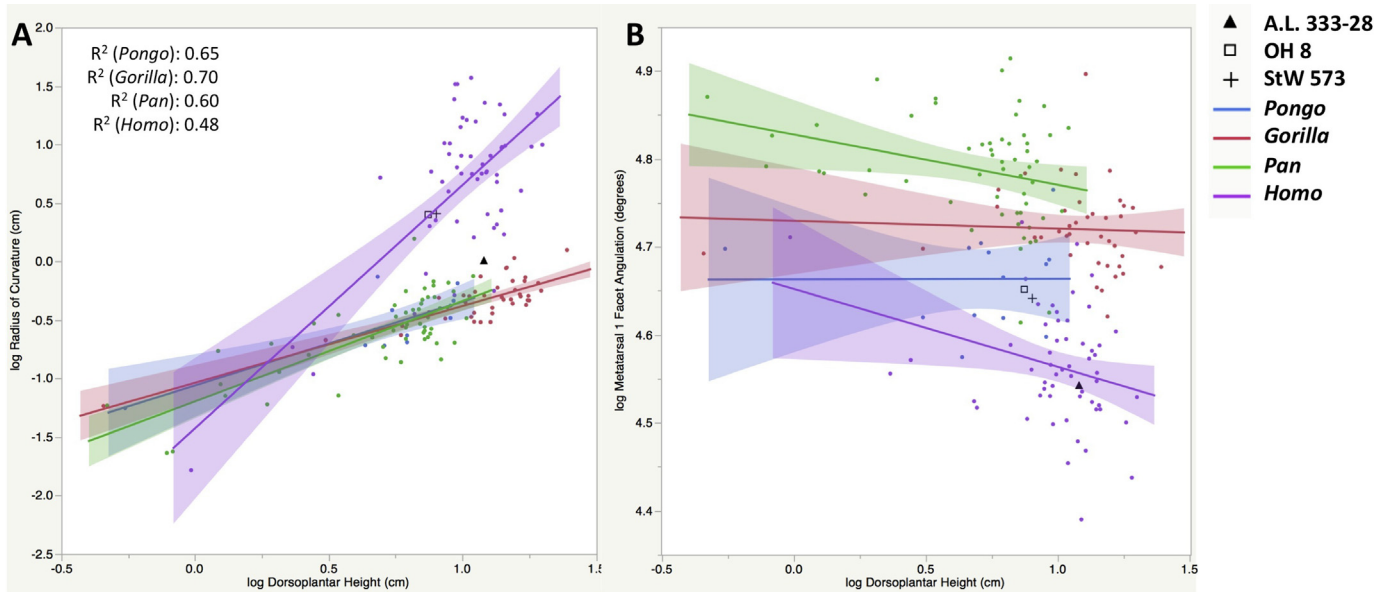
Figure 4. Bivariate regression analysis between measurements of curvature (A) and angulation (B) against dorsoplantar height. (A) Note the difference in slope magnitude between *Homo* and the extant ape species in curvature measurements. Shaded areas represent 95% confidence interval for each trend line. R^2 values are presented. (B) Note the unchanging angulation in *Gorilla* and *Pongo*, but the trend toward a less medially directed facet for the first metatarsal in both *Pan* and *Homo*. Shaded areas represent 95% confidence interval for each trend line.

was present between *Pongo* with either *Gorilla* or *Pan*. Similar to radius of curvature, angulation difference between *Pan* and *Gorilla* ($p = 0.001$) was significant, with *Pan* having the most medially angled facet. Among apes, orangutans have the least medially angled facet ($p = 0.0004$ compared to *Pan*; $p > 0.1$ compared to *Gorilla*), intermediate between *Gorilla* and *Homo* (Fig. 6).

The radius of curvature of A.L. 333-28 is outside the range of variation found in our sample of modern humans and is between the average of humans and the apes in our study. However, the orientation of the distal facet is distinctly human-like, nearly identical to the adult human mean (Tables 2 and 3). Fossils OH 8 and StW 573 are quite similar, with flatter more human-like distal facets that are more medially oriented, barely within the range of variation measured in humans (Tables 2 and 3).

4. Discussion

4.1. Ontogenetic findings

This study is the first multi-species evaluation of medial cuneiform curvature and angulation in juveniles and adults using CT (Fig. 1). A total of 170 specimens were included from extant apes,

humans, and hominins (Tables 1 and 2). We evaluated the null hypothesis that there is no alteration in curvature or angulation from birth through adulthood in extant ape and modern human medial cuneiforms. Our data refute this hypothesis, demonstrating that there are indeed significant changes that occur ontogenetically in both ape and *Homo* medial cuneiform morphology.

As described in the methods section, we quantified the osseous portion of medial cuneiforms of humans as young as 1-year-old and juvenile apes in dental stage 3 (only deciduous dentition, following Kivell and Schmitt, 2009). However, we recognize that the bones of the juvenile individuals in our study were still growing via endochondral ossification and that the shape of the preserved osteochondral interface may not mirror the shape of the joint surface, limiting any broad functional inferences. As endochondral ossification continues and the articular surface is molded through chondral modeling (Frost, 1999; Hamrick, 1999) or adaptive chondrogenesis (Hammond et al., 2010), the articular cartilage layer eventually becomes congruent with the underlying subchondral bone, allowing dry bones to be used to infer joint function. It remains unclear when this congruence occurs and thus at which developmental stage the ossification center of the medial cuneiform has matured enough to be functionally informative is

Table 3
Intraspecies comparison of medial cuneiform morphologies in extant apes and *Homo* juveniles and adults.

	Gorilla		*Pan*		*Pongo*		*Homo*	
	J	A	J	A	J	A	J	A
Radius of Curvature (cm)	0.50 ± 0.13	$0.76 \pm 0.12^*$	0.44 ± 0.14	$0.66 \pm 0.15^*$	0.53 ± 0.19	0.65 ± 0.12	1.87 ± 0.89	$2.90 \pm 1.14^*$
Metatarsal 1 facet angulation (degrees)	112.5 ± 3.6	112.3 ± 5.8	122.9 ± 5.2	$118.9 \pm 8.0^*$	105.2 ± 4.2	107.0 ± 6.9	97.5 ± 6.2	$93.4 \pm 6.0^*$
Curvature index (%)	39.6 ± 6.2	$33.8 \pm 6.3^{\ddagger}$	33.0 ± 7.6	30.3 ± 5.0	34.0 ± 8.2	40.0 ± 11.9	10.8 ± 9.9	$6.2 \pm 2.7^*$
Dorsoplantar height (cm)	1.84 ± 0.71	$3.15 \pm 0.34^{\ddagger}$	1.55 ± 0.48	$2.38 \pm 0.19^*$	1.81 ± 0.55	2.35 ± 0.35	2.65 ± 0.53	$2.98 \pm 0.29^*$

J = Juvenile; A = Adult.
Values are mean ± SD.
p-values are from log-transformed data for all measurements.
* signifies a significant intraspecies difference between juvenile and adult specimens, $p < 0.05$; ‡ denotes a trend towards significance, $0.05 \leq p < 0.1$.
An increase in the absolute value for radius of curvature measurements signifies a relatively flatter facet surface, whereas a decrease in the absolute value for the curvature index signifies a more curved facet surface.
An increase in the metatarsal 1 facet angulation denotes increased medial angulation of the facet.
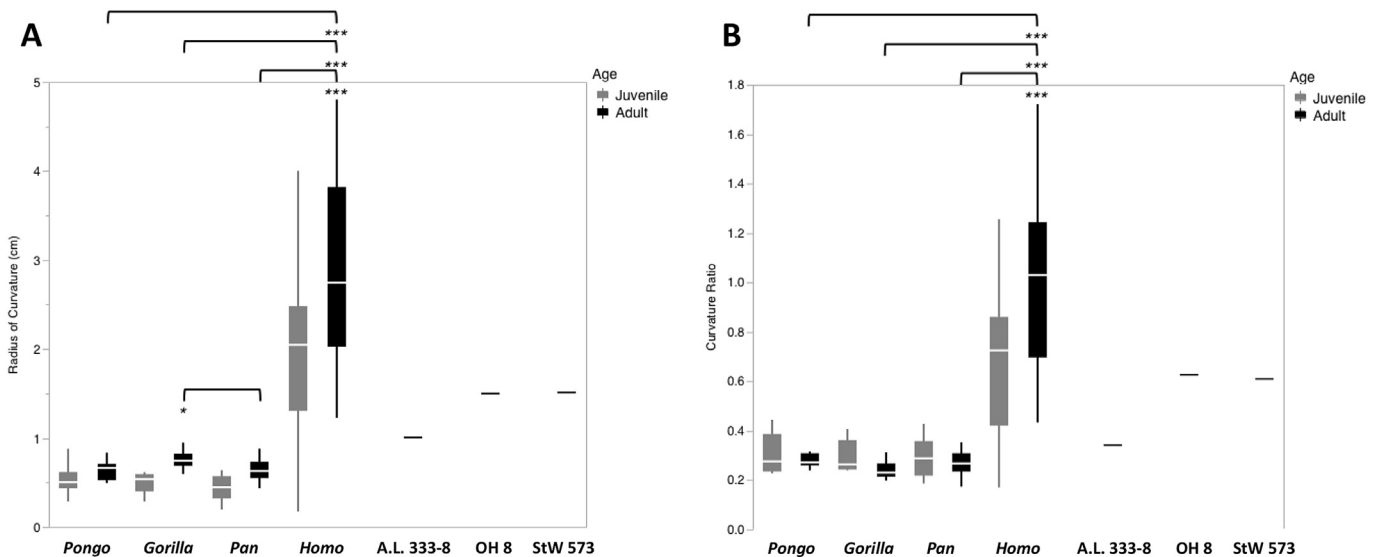
Figure 5. (A) Mean (± SD) age differences in radius of curvature. *p*-values compare adult specimens using Tukey–Kramer method. A high radius of curvature represents a flatter facet. Notice that humans have a flatter facet than the apes and that the facet flattens ontogenetically in both humans and apes. In the three hominin fossils, the facet is more convex than our modern human sample, but less convex than in apes. (B) Mean (± SD) age differences in radius of curvature standardized by dorsoplantar height. *p*-values compare adult specimens using Tukey–Kramer method. A higher curvature ratio represents a flatter facet for the first metatarsal. Notice that when standardized by size, humans still retain a flatter facet and a developmental shift from a more convex facet in juveniles to a flatter one in adults. However, this ontogenetic change is no longer apparent in the apes, meaning that they retain relatively the same convexity of the metatarsal facet as they grow. In the three hominin fossils, the facet is more convex than our modern human sample, but less convex than in apes. *** denotes $p < 0.0001$; **$p < 0.001$; *$p < 0.05$. For both Figures 5a and 5b, the box-and-whiskers plot show the median (white line), upper and lower quartiles (boxes), and range (whiskers).

uncertain. However, it is reasonable to assume that since osteogenesis is at least partially responsive to the biomechanical environment (Turner, 1998; Robling et al., 2001; Burr et al., 2002; Rath et al., 2008), a developing medial cuneiform ought to eventually achieve a shape that reflects the manner in which the tarsometatarsal joint is loaded during locomotion throughout ontogeny. In our study, we characterized the pattern by which this shape is achieved. It is notable that the youngest individuals in our sample

Figure 6. Mean (± SD) age differences in metatarsal 1 facet angulation. *p*-values compare adult specimens using Tukey–Kramer method. *p* value between *Pongo* and *Gorilla* was not significant. A higher angulation represents a more medially directed metatarsal facet on the medial cuneiform. Notice that in both humans and chimpanzees, the facet becomes more distally directed in the adults compared to the juveniles. There are also significant differences between the apes, with chimpanzees possessing the most medially directed facet, and orangutans the least. *** denotes $p < 0.0001$; **$p < 0.001$; *$p < 0.05$. The box-and-whiskers plot shows the median (white line), upper and lower quartiles (boxes), and range (whiskers).

are not outliers and instead are consistent with a developmental trend that continues through to skeletal maturity in individuals. In humans, the osteochondral surface of the first tarsometatarsal joint begins curved and flattens with age. In apes, this osseous surface also begins quite curved and that curvature is generally maintained with age.

Juvenile *Homo* medial cuneiforms have a more ape-like, convex distal surface than expected when graphed by chronological age (Fig. 3) or when standardized by the dorsoplantar height (Fig. 4a). Through developmental maturation, this surface becomes significantly flatter and there is a strong positive correlation ($R^2 = 0.78$) between distal curvature and age at time of CT scan (Fig. 3), and a positive correlation ($R^2 = 0.48$) between the flattening of the joint and osseous growth as assessed by the dorsoplantar height.

It is important to note that the medial cuneiform has been suggested to near adult morphology (but obviously not full size) by age 6 (Scheuer and Black, 2000); continued flattening of this joint after this age (Fig. 3) is instructive in how an increased stereotypic load at the first tarsometatarsal joint changes the morphology of this joint through childhood. We regard this as evidence that the hallucal tarsometatarsal joint is sensitive to the loading environment during the first decade of life as bipedalism is established and refined. A flattened facet results in a more stable hallux, which is associated with the hallmark propulsive ability of the bipedal *Homo* foot (Morton, 1935; Latimer and Lovejoy, 1990). Loss of curvature at this joint decreases the mobility of the hallux.

Additionally, in *Homo*, there was a weak negative correlation between metatarsal 1 facet angulation and dorsoplantar height. Juvenile specimens were more medially oriented than adult specimens (Fig. 4b, Table 3), though this change is subtler than the flattening that occurs at this joint. These findings are consistent with long established observations that the juvenile human foot has a more medially derived hallux (Straus, 1926; Schultz, 1926; but see Crelin, 1983). Therefore, just as there is an ontogenetic change seen in medial cuneiform curvature, there is also a change that occurs in angulation during developmental maturation in *Homo*.
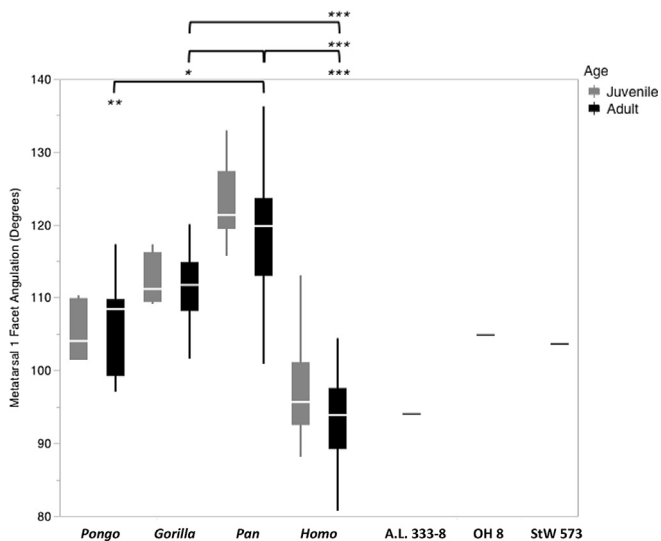
Not only does the distal medial cuneiform facet become flatter throughout ontogeny in *Homo*, but so too does it flatten in *Gorilla* and *Pan* (Table 3). However, the magnitude of change, represented by the relative regression line slopes, in medial cuneiform curvature in the extant ape specimens is considerably smaller than the accelerated morphological alteration seen in *Homo* children (Fig. 4a). Furthermore, when standardized by size, adult and juvenile apes possess the same relative curvature. Therefore, unlike in humans, the relative curvature of the distal facet of the medial cuneiform is maintained in apes, though as the ape grows, the facet mildly flattens.

A statistically significant decline in metatarsal 1 facet angulation between juveniles and adults was seen in *Pan* and *Homo*, but not in *Gorilla* or *Pongo* (Table 3). These findings may reveal an important alteration in hallucal tarsometatarsal development between the last common ancestor of the great apes and the last common ancestor between humans and chimpanzees. While the angulation of this facet appears fixed in *Gorilla* and *Pongo*, it developmentally shifts from a more medial to a more lateral position during growth of the foot in both *Pan* and *Homo*. Though the absolute magnitudes of the facet angulation are clearly distinct, the slopes for both *Homo* and *Pan* are roughly parallel, suggesting a shared pathway by which the medial cuneiform grows (Fig. 4b). While it is unclear what impact this change has on hallucal tarsometatarsal joint function in young chimpanzees, the capacity for the facet to become *less* medially angled with age may have already been present in the foot of the last common ancestor of humans and chimpanzees. A genetic change altering the initial position of the facet from being highly medially derived to slightly less medially derived (i.e., that of a juvenile *Gorilla* or *Pongo*) while maintaining the pattern of facet angulation reduction with age may have been the proximate, developmental mechanism by which hominins obtained an adducted hallux.

4.2. Adult cuneiform morphology and the hominin fossil record

As found by others (e.g., Gomberg, 1981; Latimer and Lovejoy, 1990; Harcourt-Smith, 2002), adult humans have a flatter, more distally oriented first metatarsal facet on the medial cuneiform. Difference in radius of curvature between adult *Homo*, having a flatter facet, and the adult great ape specimens were significant (Fig. 5a) even when standardized by dorsoplantar height (Fig. 5b). Additionally, differences in metatarsal 1 facet angulation between adult *Homo* and the adult great ape specimens were also significant (Fig. 6).

Interspecific analysis of the medial cuneiform across apes reveals that the great apes have different hallucal tarsometatarsal joint morphologies. *Gorilla* adult medial cuneiforms have a relatively flatter facet ($p = 0.04$) than *Pan* and, as found by others (Latimer and Lovejoy, 1990), *Pan* has the most medially angled facet for the first metatarsal. Despite being the most arboreal of the great apes, orangutans have a medial cuneiform that is the *least* medially angled, intermediate between *Gorilla* and *Homo*.

Gomberg (1981) found differences in hallucal tarsometatarsal joint morphology in *Pongo* compared to the African apes, with the former possessing high torsion of the first metatarsal facet. We too detected mediolateral torsion of the bone in the sagittal plane (see bottom left 3D reconstruction, Fig. 2) that may serve to achieve functional equivalency (a grasping hallux) in a morphologically different way than in the African great apes. Incidentally, it is this mediolateral torsion that explains the differences in our findings compared to those of Solhan (2011), who employed a plane-based approach for quantifying facet orientation. There are two possible explanations for the unique anatomy in the *Pongo* medial cuneiform. As argued by Gomberg (1981), this anatomy

may be specialized, given this species' high degree of arboreality in the context of a reduced hallux that is not as functionally important as the lateral digits during climbing (Straus, 1926; Keith, 1929; Tuttle and Rogers, 1966; Tuttle and Watts, 1985). Alternatively, this anatomy may reflect different evolutionary histories of the foot in different ape lineages from a more generalized foot in the great apes' last common ancestor (e.g., Lovejoy et al., 2009).

Our interspecific analyses on the shape of the adult medial cuneiform in apes and humans can be applied to the small sample of fossil hominin medial cuneiforms to retest hypotheses of first tarsometatarsal joint function in our ancestors and extinct relatives. Fossil hominin medial cuneiforms examined in this study fall on the edge of the human distribution (Fig. 7), though in different ways. A.L. 333-28 (*Au. afarensis*) has a more curved facet than adult modern humans, but is distinctly human-like in facet orientation. These findings mirror what Latimer and Lovejoy (1990) found. OH 8 and StW 573 have a less curved facet than A.L. 333-28, but a facet orientation that is more medially angled than most humans in this study (Fig. 4b).

While these results may be evidence for a different function of the hallucal tarsometatarsal joint in these hominins compared to modern humans, and perhaps compared to each other (Harcourt-Smith and Aiello, 2004), we caution against broad functional inferences from these data. Including smaller-bodied adult humans from an unshod, or semi-shod, population will be required before we can assert that the fossil hominin medial cuneiforms indeed fall outside the range of morphology exhibited by modern humans. Nevertheless, while the fossil hominins are on the edge of the human distribution, they are decidedly outside the range of the apes, demonstrating that the hominins represented by A.L. 333-28, OH 8, and StW 573 did not possess an ape-like opposable hallux, as many others have found for these specimens as well (Day and Napier, 1964; Latimer and Lovejoy, 1990; Harcourt-Smith and Aiello, 2004; McHenry and Jones, 2006; Lovejoy et al., 2009).

This study evaluated morphological changes from juveniles to adults in the medial cuneiform in *Homo* and extant ape species,
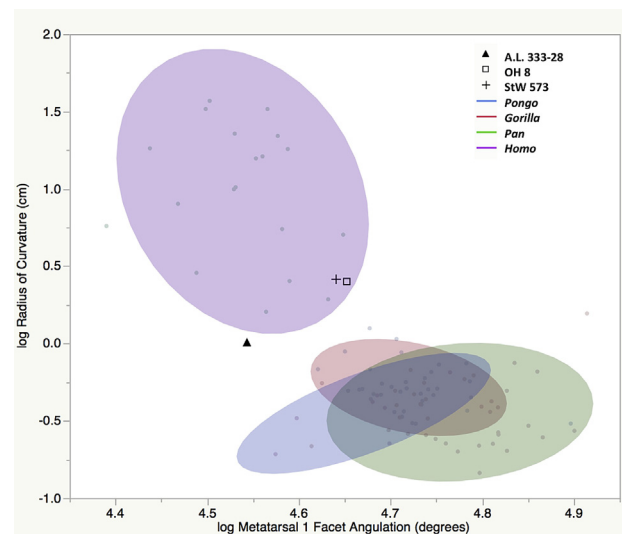

Figure 7. Bivariate density ellipses representing 90% coverage, overlaid with fossil record medial cuneiforms, between radius of curvature and metatarsal 1 facet angulation in adult extant ape and *Homo* specimens. Notice that the hominin fossils are at the edge of the human distribution with A.L. 333-28 being more convex than the humans in our study and OH 8 and StW 573 possessing more medially directed facets. However, all hominin fossils are well outside the range of variation of the ape species for these measurements.

aided by the use of CT. We determined that there is a distinct change in the medial cuneiform in *Homo* from a more medially oriented and curved distal facet in juveniles to one that is flat and only marginally angulated, helping to stabilize the push-off mechanism for bipedal locomotion. Thus, the medial cuneiform changes ontogenetically perhaps as a result of sensitivity to loading at the first tarsometatarsal joint. This pattern of ontogenetic change in both angulation and curvature of the facet is shared between chimpanzees and modern humans, but not gorillas or orangutans, which have a fixed angulation developmentally. Further work on medial cuneiforms should examine modern human populations that retain some degree of tree climbing (e.g., Venkataraman et al., 2013), especially in children, to determine whether there is an osseous signal present within these populations that correlates with some hallucal grasping during slow climbing bouts—a finding that could have important implications for arboreality in early hominins.

Disclosure

No conflict of interest.

Acknowledgments

References

Alemseged, Z., Spoor, F., Kimbel, W.H., Bobe, R., Geraads, D., Reed, D., Wynn, J.G., 2006. A juvenile early hominin skeleton from Dikika, Ethiopia. Nature 443, 296–301.

Bennett, M.W., Harris, J.W.K., Richmond, B.G., Braun, D.R., Mbua, E., Kiura, P., Olago, D., Kibunjia, M., Omuombo, C., Behrensmeyer, A.K., Huddart, D., Gonzales, S., 2009. Early hominin foot morphology based on 1.5-million-year-old footprints from Ileret, Kenya. Science 323, 1197–1201.

Berillon, G., 1999. Geometric pattern of the hominoid hallucal tarsometatarsal complex. Quantifying the degree of hallux abduction in early hominids. C.R. Acad. Sci. Paris, Série IIa 328, 627–633.

Burr, D.B., Robling, A.G., Turner, C.H., 2002. Effects of biomechanical stress on bones in animals. Bone 30, 781–786.

Clarke, R.J., Tobias, P.V., 1995. Sterkfontein Member 2 foot bones of the oldest South African hominid. Science 269, 521–524.

Crelin, E.S., 1983. The development of the human foot as a resume of its evolution. Foot Ankle Int. 3, 305–321.

Day, M.H., Napier, J.R., 1964. Fossil foot bones. Nature 201, 969–970.

Deloison, Y., 1992. Articulation cunéométatarsienne de l'hallux considérée comme un des éléments déterminants de la forme de locomotion à partir de son anatomie osseuse. Comparaison entre l'Australopithèque, l'Homme et le Chimpanzé. C.R. Acad. Sci. Paris, Série II 314, 1379–1385.

Dunn, R.H., Tocheri, M.W., Orr, C.M., Jungers, W.L., 2014. Ecological divergence and talar morphology in gorillas. Am. J. Phys. Anthropol. 153, 526–541.

Dunsworth, H.M., 2006. *Proconsul heseloni* feet from Rusinga Island, Kenya. Ph.D. Dissertation, Pennsylvania State University.

Frost, H.M., 1999. Joint anatomy, design, and arthroses: insights of the Utah paradigm. Anat. Rec. 255, 162–174.

Glard, Y., Jouve, J.-L., Panuel, M., Adalian, P., Tardieu, C., Bollini, G., 2005. An anatomical and biometrical study of the femoral trochlear groove in the human fetus. J. Anat. 206, 411–413.

Green, D.J., Alemseged, Z., 2012. *Australopithecus afarensis* scapular ontogeny, function, and the role of climbing in human evolution. Science 338, 514–517.

Gomberg, D.N., 1981. Form and function of the hominoid foot. Ph.D. Dissertation, University of Massachusetts.

Gregory, W.K., 1928. The upright posture of man: a review of its origin and evolution. Proc. Am. Philosoph. Soc. 339–377.

Hammond, A.S., Ning, J., Ward, C.V., Ravosa, M.J., 2010. Mammalian limb loading and chondral modeling during ontogeny. Anat. Rec. 293, 658–670.

Hamrick, M.W., 1999. A chondral modeling theory revisited. J. Theor. Biol. 201, 201–208.

Harcourt-Smith, W.E.H., 2002. Form and function in the hominoid tarsal skeleton. Ph.D. Dissertation, University College London.

Harcourt-Smith, W.E., Aiello, L.C., 2004. Fossils, feet and the evolution of human bipedal locomotion. J. Anat. 204, 403–416.

Jones, F.W., 1916. Arboreal man. E. Arnold, London.

Keith, A., 1923. Man's posture: its evolution and disorder. Br. Med. J. 1, 669–672.

Keith, A., 1929. The history of the human foot and its bearing on orthopaedic practice. J. Bone Joint Surg. 11, 10–32.

Kivell, T.L., Schmitt, D., 2009. Independent evolution of knuckle-walking in African apes show that humans did not evolve from a knuckle-walking ancestor. Proc. Natl. Acad. Sci. 106, 14241–14246.

Latimer, B., Lovejoy, C.O., 1990. Hallucal tarsometatarsal joint in *Australopithecus afarensis*. Am. J. Phys. Anthropol. 82, 125–133.

Latimer, B., Lovejoy, C.O., Johanson, D.C., Coppens, Y., 1982. Hominid tarsal, metatarsal, and phalangeal bones recovered from the Hadar formation: 1974–1977 collections. Am. J. Phys. Anthropol. 57, 701–719.

Lewis, O.J., 1972. The evolution of the hallucial tarsometatarsal joint in the Anthropoidea. Am. J. Phys. Anthropol. 37, 13–33.

Lovejoy, C.O., Latimer, B., Suwa, G., Asfaw, B., White, T.D., 2009. Combining prehension and propulsion: the foot of *Ardipithecus ramidus*. Science 326, 72, 72e1–72e8.

McHenry, H.M., Jones, A.L., 2006. Hallucial convergence in early hominids. J. Hum. Evol. 50, 534–539.

Midlo, C., 1934. Form of hand and foot in primates. Am. J. Phys. Anthropol. 19, 337–389.

Morton, D.J., 1935. The Human Foot: Its Evolution, Physiology, and Functional Disorders. Columbia University Press, New York.

Napier, J.R., Davis, P.R., 1959. The fore-limb skeleton and associated remains of *Proconsul africanus*. Br. Mus. Nat. Hist. Fossil Mamm. Afr. 16, 1–69.

Proctor, D.J., 2010. Brief Communication: Shape analysis of the MT 1 proximal articular surface in fossil hominins and shod and unshod *Homo*. Am. J. Phys. Anthropol. 143, 631–637.

Rath, B., Nam, J., Knobloch, T.J., Lannutti, J.J., Agarwal, S., 2008. Compressive forces induce osteogenic gene expression in calvarial osteoblasts. J. Biomech. 41, 1095–1103.

Richmond, B.G., 1998. Ontogeny and biomechanics of phalangeal form in primates. Ph.D. Dissertation, State University of New York at Stony Brook.

Robling, A.G., Duijvelaar, K.M., Geevers, J.V., Ohashi, N., Turner, C.H., 2001. Modulation of appositional and longitudinal bone growth in the rat ulna by applied static and dynamic force. Bone 29, 105–113.

Scheuer, L., Black, S.M., 2000. Developmental Juvenile Osteology. Academic Press, San Diego.

Schultz, A.H., 1926. Fetal growth of man and other primates. Quart. Rev. Biol. 1, 465–521.

Schultz, A.H., 1930. The skeleton of the trunk and limbs of higher primates. Hum. Biol. 2, 303–438.

Schultz, A.H., 1934. Some distinguishing characters of the mountain gorilla. J. Mammal. 15, 51–61.

Shefelbine, S.J., Tardieu, C., Carter, D.R., 2002. Development of the femoral bicondylar angle in hominid bipedalism. Bone 30, 765–770.

Solhan, C.R., 2011. Hallucial tarsometatarsal joint morphology and function: a three-dimensional analysis of medial cuneiforms in extant and fossil hominids. Masters Thesis, The George Washington University.

Stern, J.T., Susman, R.L., 1983. The locomotor anatomy of *Australopithecus afarensis*. Am. J. Phys. Anthropol. 60, 279–317.

Straus, W.L., 1926. The development of the human foot and its phylogenetic significance. Am. J. Phys. Anthropol. 9, 427–438.

Susman, R.L., 1983. Evolution of the human foot: evidence from Plio-Pleistocene hominids. Foot Ankle Int. 3, 365–376.

Susman, R.L., Stern, J.T., Jungers, W.L., 1984. Arboreality and bipedality in the Hadar hominids. Folia Primatol. 43, 113–156.

Tardieu, C., 1999. Ontogeny and phylogeny of femoro-tibial characters in humans and hominid fossils: functional inference and genetic determinism. Am. J. Phys. Anthropol. 110, 365–377.

Tardieu, C., 2010. Development of the human hind limb and its importance to the evolution of bipedalism. Evol. Anthropol. 19, 174–186.

Tocheri, M.W., Solhan, C.R., Orr, C.M., Femiani, J., Frohlich, B., Groves, C.P., Harcourt-Smith, W.E., Richmond, B.G., Shoelson, B., Jungers, W.L., 2011. Ecological divergence and medial cuneiform morphology in gorillas. J. Hum. Evol. 60, 171–184.

Turner, C.H., 1998. Three rules for bone adaptation to mechanical stimuli. Bone 23, 399–407.

Tuttle, R.H., Rogers, C.M., 1966. Genetic and selective factors in reduction of the hallux in *Pongo pygmaeus*. Am. J. Phys. Anthropol. 24, 191–198.

Tuttle, R.H., Watts, D.P., 1985. The positional behavior and adaptive complexes of *Pan gorilla*. In: Kondo, S., Ishida, S., Okada, M., Kimura, T., Yamazaki, M. (Eds.), Primate Morphophysiology, Locomotor Analyses and Human Bipedalism. Tokyo University Press, Tokyo, pp. 261–288.

Tyson, E., 1699. Orang-Outang, Sive *Homo sylvestris*: or, the Anatomy of a Pygmie Compared with that of a Monkey, an Ape, and a Man. Dawsons of Pall Mall, London.

Venkataraman, V.V., Kraft, T.S., Dominy, N.J., 2013. Tree climbing and human evolution. Proc. Natl. Acad. Sci. 110, 1237–1242.

Ward, C.V., 2002. Interpreting the posture and locomotion of *Australopithecus afarensis*: where do we stand? Am. J. Phys. Anthropol. 119, 185–215.

Weidenreich, F., 1923. Evolution of the human foot. Am. J. Phys. Anthropol. 6, 1–10.

Zollikofer, C.P.E., Ponce de León, M.S., 2013. Pandora's growing box: inferring the evolution and development of hominin brains from endocasts. Evol. Anthropol. 22, 20–33.